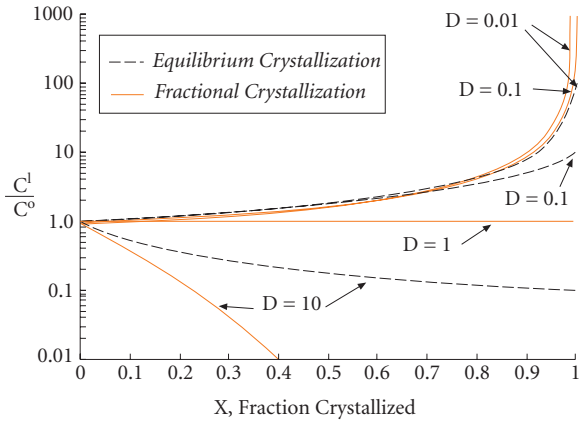

Figure 7.29 Variation of relative trace element concentration in a liquid undergoing crystallization.

elements would have partition coefficients close to 1 for such an acid melt.* This limits the enrichment of incompatible elements. However, highly *compatible* elements (elements with solid/liquid partition coefficients greater than 1, such as Ni) do have concentrations that approach 0 in fractionated melts (generally they disappear below detection limits). Variation of relative trace element concentration as a function of the fraction of liquid remaining is shown in Figure 7.29.

In summary, for moderate amounts of fractionation, crystallization has only a moderate effect on trace element concentrations, given that these concentrations vary by orders of magnitude.

7.7.3 *In situ* crystallization

A magma chamber is likely to be substantially hotter than the rock surrounding it, which will result in a substantial thermal gradient at the margin of the chamber. Thus the margins, particularly the roof and walls, are likely to be cooler than the interior, and it is here where crystallization will primarily occur. Crystals sloughed from the walls and roof would accumulate on the floor. When crystallization is restricted to marginal zones of the chamber, magma composition will evolve in a somewhat different manner than for simple fractional crystallization. Langmuir (1989) called this process *in situ crystallization*.

Imagine a magma chamber that is bounded by a zone of well-consolidated crystals at the margin. There may be some liquid within this zone, but we assume that the permeability is sufficiently low that it will never return to the magma chamber. Between this "cumulate zone" and the free magma is a transition zone of higher permeability, which we call the "solidification zone" (Figure 7.30). Magma is added to the solidification zone as crystallization advances into the chamber. As crystallization and compaction proceed within the solidification zone, liquid is expelled back into the central magma. The flux of magma to the solidification zone we will designate dM_I and the return flux as dM_A. We let f be the fraction of interstitial liquid remaining after crystallization within the solidification zone, and $(1 - f)$ be fraction of liquid crystallized within this zone. Some fraction f_T of the liquid remains to form the trapped liquid within the cumulate zone, and some fraction f_A returns to the magma, so that $f = f_T + f_A$. Hence:

$$dM_A = f_A dM_I \tag{7.83}$$

If the magma plus cumulates form a closed system, then the change in mass of liquid within the chamber is the difference between the flux into and out of the solidification zone:

$$dM_L = dM_A - dM_I = dM_I(f_A - 1) \tag{7.84}$$

If C_L is the concentration of some element in the magma and C_f is the concentration in the liquid returning from the solidification zone, then the change in mass of the element is:

$$\begin{aligned} d(M_L C_L) &= C_L dM_L + M_L dC_L \\ &= C_f dM_A - C_L dM_I \end{aligned} \tag{7.85}$$

We define the parameter E as the ratio of the concentration in the magma to that in the returning liquid:

* Silica-rich, or silicic, melts are sometimes referred to as "acidic" and Mg- and Fe-rich ones as "basic". The reason is historical: it was once thought that silica was present in melts as H_4SiO_4. This is not the case, but the terminology persists.

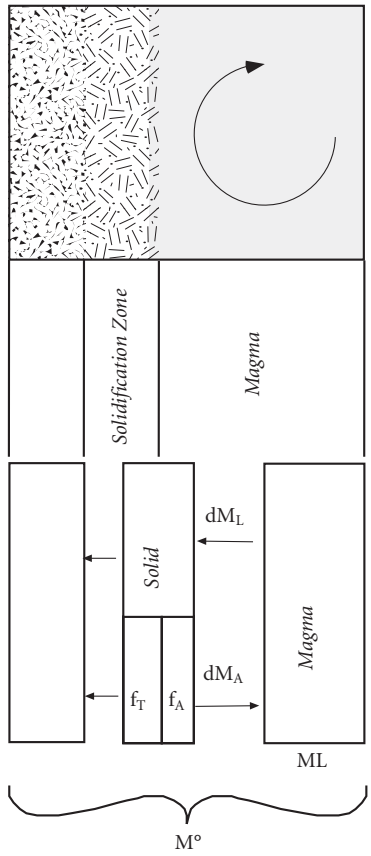

Figure 7.30 Cartoon of magma chamber undergoing *in situ* crystallization. The solidification zone is the transition region between consolidated cumulates (that nevertheless retain some trapped liquid) and the magma chamber. As crystallization proceeds, some liquid will be expelled from the solidification zone back into the magma. Adapted from Langmuir (1989).

$$E = C_f / C_L \tag{7.86}$$

E will depend upon the partition coefficient for the element of interest and on the manner in which crystallization proceeds within the solidification zone. If, for example, we assume that there is complete equilibration between crystals and liquid within the zone, then from eqn. 7.81:

$$E = \frac{1}{D(1-f)+f} \tag{7.87}$$

Substituting eqns. 7.83, 7.85, and 7.86 into 7.84 and rearranging, we have:

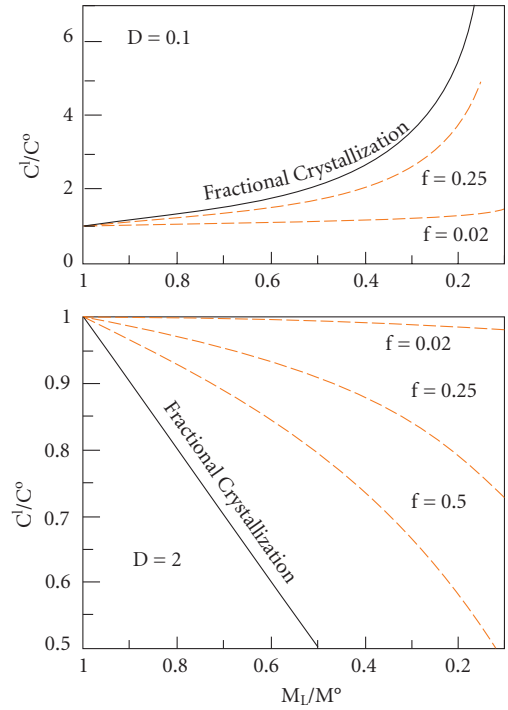

Figure 7.31 Comparison of the effects of *in situ* and fractional crystallization on concentration for two values of the distribution coefficient, D, and several values of *f*. f_A is assumed to equal *f* (i.e., no trapped liquid remains in the cumulate zone). Adapted from Langmuir (1989).

$$\frac{dC_L}{C_L} = \frac{dM_L}{M_L}\left(\frac{f_A(E-1)}{f_A - 1}\right) \tag{7.88}$$

Assuming E and f_A are constants, we can integrate eqn. 7.88 to yield:

$$\frac{C_L}{C^0} = \left(\frac{M_L}{M^0}\right)^{f_A(E-1)/(f_A-1)} \tag{7.89}$$

Figure 7.31 compares the change in concentration due to *in situ* crystallization and fractional crystallization for two values of D and several values of *f*. In general, *in situ* crystallization results in less enrichment of incompatible elements and less depletion of compatible elements for a given degree of crystallization of a magma body than does fractional crystallization. The degree of enrichment depends upon *f*, the fraction of liquid remaining when liquid is expelled from

the solidification zone. For very small values of f, that is, complete crystallization within the solidification zone, the composition of the magma remains nearly constant. For $f = 1$, that is, for no crystallization within the solidification zone, eqn. 7.89 reduces to eqn. 7.82, and the *in situ* curves in Figure 7.31 coincide with the fractional crystallization curves.

7.7.4 Crystallization in open system magma chambers

Thus far, we have treated crystallization only in closed systems, that is, where a certain volume of magma is intruded and subsequently cools and crystallizes without withdrawal or further addition of magma. This is certainly not a very realistic model of magmatism and volcanism. In the well-studied Hawaiian volcanoes for example, injections of new magma into crustal magma chambers are fairly frequent. Indeed, it appears that addition of magma to the Kilauean magma chamber is nearly continuous. Furthermore, many igneous rocks show petrographic evidence of mixing of differentiated magmas with more primitive ones. In this section, we consider the concentrations of trace elements in open magma chambers; that is, the case where new "primary" magma mixes with a magma that has already undergone some fractional crystallization. Magma chambers where crystallization, eruption and addition of new magma occur are sometimes called RTF magma chambers, the RTF referring to "refilled", "tapped", and "fractionated".

The extreme case of an RTF magma chamber is a *steady-state* system, where the magma resupply rate equals the rate of crystallization and eruption, thus maintaining a constant volume of liquid (Figure 7.32). In such a magma chamber, the concentrations of all elements eventually reach steady state after many cycles of refilling, eruption, and fractional crystallization. Steady state occurs when the rate of supply of the elements (due addition of new magma) becomes equal to the rate of loss (due to crystallization and withdrawal and eruption of magma).

To understand how steady-state is achieved, consider a cyclic process where a volume C is lost by crystallization and a volume T is lost by eruption and a volume $(T + C)$ is added to the magma chamber during each cycle. For

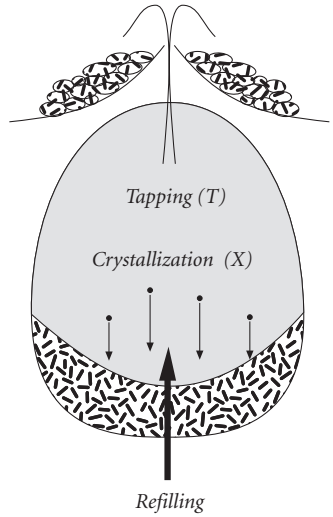

Figure 7.32 Schematic illustration of a steady-state and periodically refilled, fractionally crystallized, and tapped magma chamber beneath a mid-ocean ridge.

incompatible elements, the concentration in the liquid initially increases because a greater mass of these elements is added by refilling than is lost by crystallization and eruption. As the concentration in the liquid increases, so does the concentration in the solid since $C^s = D^{s/l} C^l$ ($D^{s/l}$ would be a bulk distribution coefficient if more than one phase is crystallizing). Eventually a point is reached where the concentration in the solid is so great, that loss of the element by crystallization and eruption equals the gain resulting from refilling.

We can quickly derive an expression for the steady-state concentration of an element in the *equilibrium crystallization* case. In steady-state, the losses of an element must equal gains of that element, so:

$$C°(X + T) = TC^{ssl} + XC^s \qquad (7.90)$$

where $C°$ is the concentration in the primary magma being added to the chamber, C^{ssl} is the concentration in the steady-state liquid, and C^s is the concentration in the solid. Since $C^s = D^{s/l}C^{ssl}$:

$$C°(X + T) = TC^{ssl} + XDC^{ssl} \qquad (7.91)$$

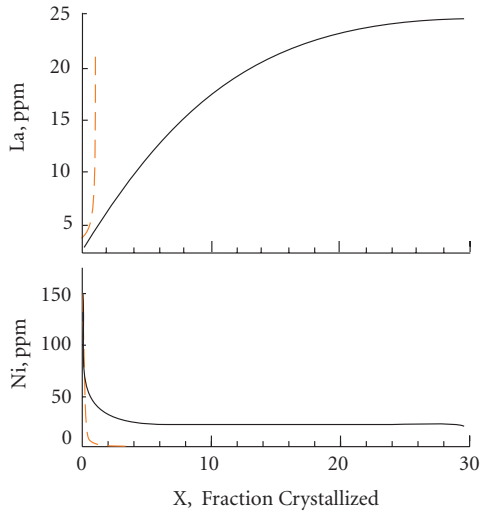

Figure 7.33 Concentration of Ni and La in closed system fractional crystallization (dashed line) and open system crystallization (solid line) as a function of the fraction crystallized. In the open system case the mass injected into the chamber is equal to the mass crystallized (i.e., Y = 0).

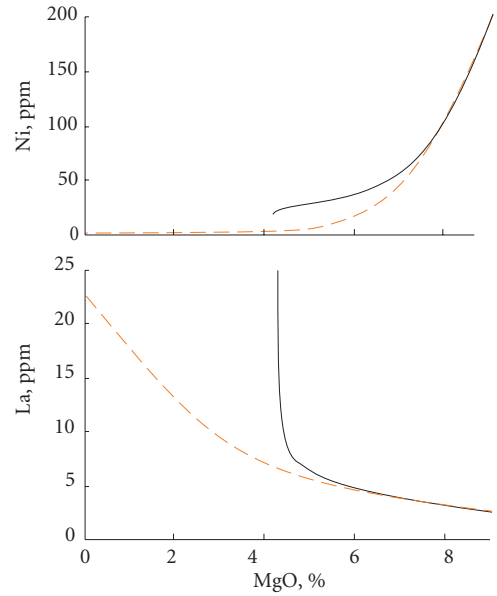

Figure 7.34 La and Ni concentrations plotted against MgO concentration in a basalt undergoing closed system fractional crystallization (dashed red line) and in a steady-state magma chamber where the mass of new magma equals the mass crystallized in each cycle (solid line).

We can rearrange this to obtain the enrichment in the steady-state liquid relative to the primary magma:

$$\frac{C^{ssl}}{C^0} = \frac{X+T}{X+TD^{s/l}} \qquad (7.92)$$

For the fractional crystallization case, the enrichment factor is:

$$\frac{C^{ssl}}{C^0} = \frac{(X+T)(1-X)^{D-1}}{1-(1-X-T)(1-X)^{D-1}} \qquad (7.93)$$

These equations are from O'Hara (1977).

Compatible element concentrations reach steady-state after fewer cycles than do incompatible elements. This is illustrated in Figure 7.33, which shows how the concentrations of La, an incompatible element, and Ni, a compatible element, vary as a function of the total amount crystallized in a steady-state system. The Ni concentration, which is 200 ppm in the primary magma, reaches a steady-state concentration of about 20 ppm after the equivalent of 5 magma chamber masses has crystallized. After the equivalent of 30 magma chamber masses crystallization, La has not quite reached its steady-state concentration of around 25 ppm.

Unfortunately, it is never possible to measure the fraction of magma that has crystallized. In place of our parameter, X, petrologists often use the concentration of some "index species", i.e., some species whose behavior is relatively well understood and whose concentration should vary smoothly as a function of the fraction crystallized. In basalts, MgO is commonly used as the index species, while SiO_2 is a more common index in more acidic magmas such as andesites and dacites. Figure 7.34 shows the La and Ni concentrations against the MgO concentration in the same steady-state system. Since MgO is a compatible element (though not a trace element, we could treat it using the same equations we have derived for trace elements), it quickly reaches a steady-state concentration at around 4.25%, while the La concentration continues to increase. Lavas erupted from this magma chamber could thus have essentially

constant MgO and Ni concentrations, but variable La concentrations. This apparent "decoupling" of compatible and incompatible element concentrations is a feature of open magmatic systems.

7.8 SUMMARY OF TRACE ELEMENT VARIATIONS DURING MELTING AND CRYSTALLIZATION

For moderate amounts of crystallization, fractional crystallization does not have dramatic effects on *incompatible* element concentrations. Concentrations of highly *compatible* elements are, however, dramatically affected by fractional crystallization. The RTF model does have significantly greater effects on incompatible element concentrations than simpler models, however.

Partial melting has much more dramatic effects on *incompatible* element concentrations. It is likely that much of the incompatible element variations observed in magmas and magmatic rocks are related to variations in degree of melting. Depth of melting also has an effect, in that the phases with which melts equilibrate vary with depth. For example, the presence of garnet dramatically affects rare earth element (REE) abundances. The heavy rare earths are accepted into the garnet structure and have Ds > 1. The lights are, however, highly rejected. The presence of garnet in the partial melting residua can thus lead to strong light rare earth enrichment of the melt.

Two simplifications are important for partial melting (both batch and fractional). *When D << F, the enrichment is 1/F*. Thus for small D, the enrichment is highly dependent on the degree of melting. If D is large (i.e., D > 1 and D >> F), the depletion of the element in the melt is rather insensitive to F. In either case, *when F approaches 0, the maximum enrichment or depletion is 1/D*.

Highly *compatible* elements are, of course, depleted in a partial melt. But the degree of depletion is rather insensitive to the degree of melting for values of F likely to occur in the mantle (<0.25). It must be emphasized that we have no good constraints on the absolute values of F.

This all works out nicely: *compatible elements are good qualitative indicators of the extent of fractional crystallization and incompatible elements are good indicators of the degree of melting*.

Both geochemical and (experimental) petrological evidence indicates that alkali basalts and their kin are the result of lower degrees of melting than tholeiites. Highly undersaturated rocks such as nephelinites are probably produced by the smallest degrees of melting (1% or less). At the same time, alkali basalts are probably also the products of deeper melting.

Ratios of incompatible elements are generally less sensitive to fractional crystallization and partial melting than are absolute abundances, particularly if they are of similar incompatibility. For relatively large extents of melting, the ratio of two incompatible ele-

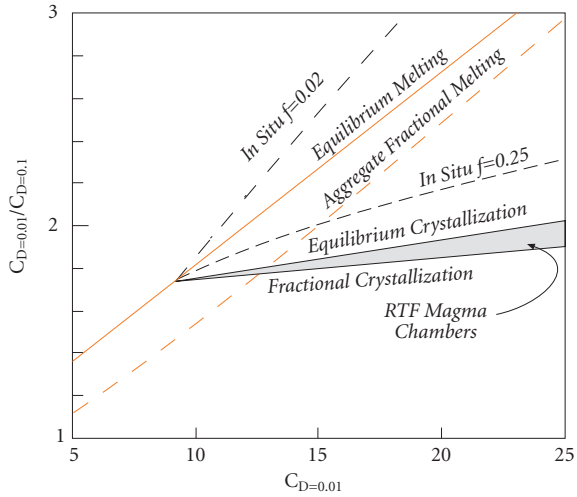

Figure 7.35 Plot of the ratio of two incompatible elements (one with D = 0.01, the other with D = 0.1) versus the concentration of the more incompatible element. The plot shows calculated effects of equilibrium partial melting and aggregate partial melting, assuming concentrations of 1 in the source for both elements. Other lines show the effect of crystallization on the composition of a liquid produced by 10% equilibrium melting. Fractional crystallization, equilibrium crystallization, and open system crystallization (RTF magma chambers) produce less variation of the ratio than does partial melting. *In situ* crystallization can mimic the effect of partial melting if the value of *f*, the fraction of liquid returned to the magma, is sufficiently small.

ments in a magma will be similar to that ratio in the magma source. For this reason, trace element geochemists are often more interested in the ratios of elements than in absolute abundances.

One approach commonly used is to plot the ratio of two incompatible elements against the abundance of the least compatible of the two. This kind of plot is sometimes referred to as a *process identification plot* because fractional crystallization and partial melting result in very different slopes on such a diagram. Figure 7.35 is a schematic version of a process identification plot. Crystallization, both fractional and equilibrium, produce rather flat slopes on such a diagram, as does crystallization in an open system magma chamber. Partial melting produces a much steeper slope and the slope produced by aggregates of fractional melts is similar to that of equilibrium partial melting. *In situ* crystallization can produce a range of slopes depending on the value of f. Langmuir (1989) found that a value for f of 0.25 best matched the variation observed in the Kiglapait Intrusion in Labrador, a classic large layered intrusion. Assuming this value of f is typical, then the change in a trace element ratio due to *in situ* crystallization should be only moderately greater than for fractional crystallization.

REFERENCES AND SUGGESTIONS FOR FURTHER READING

Albarède, F. 1995. *Introduction to Geochemical Modeling*. Cambridge, Cambridge University Press.

Azimov, P.D., Hirschmann, M.M. and Stolper, E. 1997. An analysis of variations in isoentropic melt productivity. *Philosophical Transactions of the Royal Society London A*, 355: 255–81.

Barnes, S.-J., Naldrett, A.J. and Gorton, M.P. 1985. The origin of the fractionation of platinum-group elements in terrestrial magmas. *Chemical Geology*, 53: 303–23.

Beattie, P. 1993. Olivine-melt and orthopyroxene-melt equilibria. *Contributions to Mineralogy and Petrology*, 115: 103–11.

Beattie, P. 1994. Systematics and energetics of trace-element partitioning between olivine and silicate melts: implications for the nature of mineral/melt partitioning. *Chemical Geology*, 117: 57–71.

Beattie, P., Drake, M., Jones, J., *et al*. 1993. Terminology for trace-element partitioning. *Geochimica et Cosmochimica Acta*, 57: 1605–6.

Ben Othman, D., White, W.M. and Patchett, J. 1989. The geochemistry of marine sediments, island arc magma genesis, and crust-mantle recycling. *Earth and Planetary Science Letters*, 94: 1–21.

Blundy, J.D., Robinson, J.C. and Wood, B.J. 1998. Heavy REE are compatible in clinopyroxene on the spinel lherzolite solidus. *Earth and Planetary Science Letters*, 160: 493–504.

Blundy, J. and Wood, B. 1994. Prediction of crystal-melt partition coefficients from elastic moduli. *Nature*, 372: 452–4.

Blundy, J. and Wood, B. 2003. Partitioning of trace elements between crystals and melts. *Earth and Planetary Science Letters*, 210: 383–97.

Brice, J.C. 1975. Some thermodynamic aspects of the growth of strained crystals. *Journal of Crystal Growth*, 28: 249–53.

Brügmann, G.E., Arndt, N.T., Hofmann, A.W. and Tobschall, H.J. 1987. Noble metal abundances in komatiite suites from Alexo, Ontario, and Gorgona Island, Columbia. *Geochimica et Cosmochimica Acta*, 51: 2159–71.

Brügmann, G.E., Naldrett, A.J., Asif, M., *et al*. 1993. Siderophile and chalcophile metals as tracers of the evolution of the Siberian Trap in the Noril'sk region, Russia. *Geochimica et Cosmochimica Acta*, 57: 2001–18.

Burns, R.G. 1970. *Mineralogical Applications of Crystal Field Theory*. Cambridge, Cambridge University Press.

Burns, R.G. 1973. The partitioning of trace transition elements in crystal structures: a provocative review with applications to mantle geochemistry. *Geochimica et Cosmochimica Acta*, 37: 2395–2403.

Carroll, M.R. and Draper, D.S. 1994. Noble gases as trace elements in magmatic processes. *Chemical Geology*, 117: 37–56.

Drake, M.J. and Weill, D.F. 1975. Partition of Sr, Ba, Ca, Y, Eu^{2+}, Eu^{3+}, and other REE between plagioclase feldspar and magmatic liquid: an experimental study. *Geochimica et Cosmochimica Acta*, 39, 689–712.

Elderfield, H. and Greaves, M.J. 1982. The rare earth elements in seawater. *Nature*, 296: 214–19.

Fryer, B.J. and Greenough, J.D. 1992. Evidence for mantle heterogeneity from platinum-group element abundances in Indian Ocean basalts. *Canadian Journal of Earth Sciences*, 29: 2329–40.

Gallahan, W.E. and Nielsen, R.L. 1992. The partitioning of Sc, Y and the rare earth elements between high-Ca pyroxene and natural mafic to intermediate lavas at 1 atmosphere. *Geochimica et Cosmochimica Acta*, 56: 2387–404.

Hack, P.J., Nielsen, R.L. and Johnston, A.D. 1994. Experimentally determined rare-earth element and Y partitioning behavior between clinopyroxene and basaltic liquids at pressures up to 20 kbar. *Chemical Geology*, 117: 89–105.

Harrison, W.J. 1979. Rare earth elements partitioning between garnet lherzolite minerals and melts during partial melting. *Carnegie Institute of Washington Yearbook*, 78: 562–8.

Hart, S.R. 1993. Equilibration during mantle melting: a fractal tree model. *Proceedings of the National Academy of Sciences USA*, 90: 11914–18.

Hiemstra, S.A. 1979. The role of collectors in the formation of platinum deposits in the Bushveld Complex. *Canadian Mineralogist*, 17: 469–82.

Jochum, K.-P., Hofmann, A.W. and Seifert, H.M. 1985. Sn and Sb in oceanic basalts and the depletion of the siderophile elements in the primitive mantle (abs). *EOS*, 66: 1113.

Jochum, K.-P., Hofmann, A.W. and Seifert, H.M. 1993. Tin in mantle-derived rocks: Constraints on Earth evolution. *Geochimica et Cosmochimica Acta*, 57: 3585–95.

Jones, J.H. 1995. Experimental trace element partitioning, in *Rock Physics and Phase Relations: a Handbook of Physical Constants, AGU Reference Shelf 3* (ed. T.J. Ahrens), pp. 73–104. Washington, American Geophysical Union.

Kingery, W.D. 1960. *Introduction to Ceramics*. New York, John Wiley and Sons, Ltd.

Kohlstedt, D.L. 1993. Structure, rheology and permeability of partially molten rocks at low melt fractions, in *Mantle Flow and Melt Generation at Mid-ocean Ridges, Geophysical Monograph 71* (eds J.P. Morgan, D.K. Blackman and J.M. Sinton), pp. 103–21. Washington, American Geophysical Union.

Kohn, S.C. and Schofield, P.F. 1994. The implication of melt composition in controlling trace-element behavior: an experimental study of Mn and Zn partitioning between forsterite and silicate melts. *Chemical Geology*, 117: 73–87.

Langmuir, C.H. 1989. Geochemical consequences of *in situ* crystallization. *Nature*, 340: 199–205.

Langmuir, C.H., Klein, E.M. and Plank, T. 1993. Petrological systematics of mid-ocean ridge basalts: constraints on melt generation beneath oceanic ridges, in *Mantle Flow and Melt Generation at Mid-ocean Ridges, Geophysical Monograph 71* (eds J.P. Morgan, D.K. Blackman and J.M. Sinton), pp. 183–280. Washington, American Geophysical Union.

Laporte, D. 1994. Wetting behavior of partial melts during crustal anatexis: the distribution of hydrous silicic melts in polycrystalline aggregates of quartz. *Contributions to Mineralogy and Petrology*, 116: 486–99.

Masuda, A. and Nakamura, N. 1973. Fine structures of mutually normalized rare-earth patterns of chondrites. *Geochimica et Cosmochimica Acta*, 37: 239–48.

McClure, D.S. 1957. The distribution of transition metal cations in spinel. *J. Phys. Chem. Solids*, 3: 311–17.

McLennan, S.M. 1989. Rare earth elements in sedimentary rocks: influence of provenance and sedimentary processes, in *Geochemistry and Mineralogy of the Rare Earths, Reviews in Mineralogy 21* (eds B.R. Lipin and G.A. McKay), pp. 169–200. Washington, Mineralogical Society of America.

Mitchell, R.H. and Keays, R.R. 1981. Abundance and distribution of gold, palladium and iridium in some spinel and garnet lherzolites: implications for the nature and origin of precious metal-rich intergranular components in the upper mantle. *Geochimica et Cosmochimica Acta*, 45: 2425–42.

Morgan, J.P. 2001. Thermodynamics of pressure release melting of a veined plum pudding mantle. *Geochem. Geophys. Geosyst.*, 2: paper no. 2002GC000049.

Nakamura, N. 1974. Determination of REE, Ba, Fe, Mg, Ba, and K in carbonaceous and ordinary chondrites. *Geochimica et Cosmochimica Acta*, 38: 7577–775.

Naldrett, A.J., Hoffman, E.L., Green, A.H., Chou, C.L. and Naldrett, S.R. 1979. The composition of Ni-sulfide ores with particular reference to their content of PGE and Au. *Canadian Mineralogist*, 17: 403–15.

Newsom, H.E., White, W.M., Jochum, K.P. and Hofmann, A.W. 1986. Siderophile and chalcophile element abundances in oceanic basalts, Pb isotope evolution and growth of the Earth's core. *Earth and Planetary Science Letters*, 80: 299–313.

Nielsen, R.L. and Dungan, M.A. 1983. Low pressure mineral–melt equilibria in natural anhydrous mafic systems. *Contributions to Mineralogy and Petrology*, 84: 310–26.

O'Hara, M.J. 1977. Geochemical evolution during fractional crystallization of a periodically refilled magma chamber. *Nature*, 266: 503–7.

O'Hara, M.J. 1985. Importance of the 'shape' of the melting regime during partial melting of the mantle. *Nature*, 314: 58–62.

Onuma, N., Higuchi, H., Wakita, H. and Nagasawa, H. 1968. Trace element partition between two pyroxenes and the host lava. *Earth and Planetary Science Letters*, 5: 47–51.

Orgel, L.E. 1966. *An Introduction to Transition Metal Chemistry: Ligand Field Theory*. London, Methuen.

Palme, H. and Jones, A. 2005. *Solar system abundances of the elements, in Meteorites, Comets, and Planets, Treatise on Geochemistry, vol. 1* (ed. A.M. Davis), pp. 41–62. Amsterdam, Elsevier.

Piper, D.Z. 1974. Rare earth elements in the sedimentary cycle: a summary. *Chemical Geology* 14: 285–304.
Plank, T. and Langmuir, C.H. 1992. Effects of the melting regime on the composition of the oceanic crust. *Journal of Geophysical Research*, 97: 19749–70.
Riley, G.N. and Kohlstedt, D.L. 1990. Kinetics of melt migration in upper mantle-type rocks. *Earth and Planetary Science Letters*, 105: 500–21.
Rollinson, H. 1993. *Using Geochemical Data: Evaluation, Presentation, Interpretation*. Essex, Longman Scientific and Technical.
Rudnick, R.R. and Fountain, D.M. 1995. Nature and composition of the continental crust: a lower crustal perspective. *Reviews in Geophysics*, 33: 267–309.
Shaw, D.M. 1970. Trace element fractionation during anatexis. *Geochimica et Cosmochimica Acta*, 34: 237–43.
Stockman, H.W. 1982. *Noble metals in the Ronda and Josephine peridotites*, PhD dissertation. Cambridge, MIT.
Taylor, S.R., and McLennan, S.M. 1985. *The Continental Crust: its Composition and Evolution*. Oxford, Blackwell Scientific.
Watson, E.B. 1976. Two-liquid partition coefficients: experimental data and geochemical implications. *Contributions to Mineralogy and Petrology*, 56: 119–34.
Wood, B.J., Blundy, J.D. and Robinson, J.C. 1999. The role of clinopyroxene in generating U-series disequilibrium during mantle melting. *Geochimica et Cosmochimica Acta*, 63: 1613–20.
Zhou, M.-F. 1994. PGE distribution in 2.7-Ga layered komatiite flows from the Belingwe greenstone belt, Zimbabwe. *Chemical Geology*, 118: 155–72.

PROBLEMS

1. For one element not in the groups described in Section 7.2.2 (Mo, W, Ag, Cd, P, In, Sn, Tl, or Bi), write several paragraphs on its geochemistry. Include answers to the following: what valence state (or states) will it have in nature? What is its ionic radius in its most common valence state (preferably in octahedral coordination)? What is its electronegativity? What kinds of bonds will it most likely form? How will it behave, in particular what is its solubility, in aqueous solution? What element will it most easily substitute for in silicate rocks? Is it volatile or does it form volatile compounds? Is it siderophile or chalcophile? Will it behave as a compatible or incompatible element? What are its uses? What are the primary sources of the element for use by man?

2. Make rare earth plots for the following two samples. For the granite, plot it normalized to one of the chondritic values in Table 7.3. For the Mn nodule, make one plot normalizing it to chondrites and one plot normalizing it to average shale. Describe the features of the REE patterns.

	La	Ce	Pr	Nd	Sm	Eu	Gd	Tb	Dy	Ho	Er	Tm	Yb	Lu
Granite	41	75		25	3.6	0.6	2.7		1.3				0.4	
Mn nodule	110	858		116	24	4.9	24		24.1		14.4		13	1.92

3. Using the Blundy and Wood model, calculate the partition coefficients for the alkali metals in plagioclase at 1250°C. Assume that the site radius in 124 nm and that an ion of this radius would have a partition coefficient of 1. Assume that the value of Young's modulus in plagioclase is 64 GPa and that ionic radii for the alkalis are as follows: Li: 76 pm, Na 102 pm, K 138 pm, Rb 152 pm, and Cs 167 pm.

4. Relatively Ca-rich garnets (i.e., grossular-rich) appear to accept high field strength elements in both the X (normally occupied by Ca^{2+}, Mg^{2+}, Fe^{2+}, etc.) and Y (normally occupied by Al^{3+}, Fe^{3+}, etc.) crystallographic sites. The garnet/liquid partition coefficient should be the sum of the individual partition coefficients for each site. Assume that D_0, r_o, and E for the X site are 7, 91 pm and 1350 GPa respectively, and the corresponding values for the Y site are 1.9, 67 pm, and 920 GPa respectively. Ions in the X site will be in 8-fold coordination,

while ions in the Y site will be in 6-fold coordination. In 8-fold coordination, the ionic radii of Zr^{4+}, Hf^{4+}, Th^{4+}, and U^{4+} are 84 pm, 83 pm, 105 pm, and 100 pm respectively; in 6-fold coordination they will be 72 pm, 71 pm, 94 pm, and 89 pm respectively. Calculate the garnet/liquid partition coefficients for these four elements at 1250°C using the Blundy and Wood model.

5. Does Gallahan and Nielsen's (1992) equation for the cpx/liquid partition coefficient (eqn. 7.31) have the form you expect from thermodynamics? If so, what does the *a* parameter represent? What does the *b* parameter represent? Derive this equation from the thermodynamic relationships we developed in Chapter 3.

6. Calculate the cpx/melt partition coefficients for La and Sm using the method of Gallahan and Nielsen (1992) for the following basalt from Reunion Island:

SiO_2	46.99
TiO_2	2.66
Al_2O_3	13.57
Fe_2O_3	13.38 (total Fe as Fe_2O_3)
MnO	0.18
MgO	9.78
CaO	9.51
Na_2O	2.91
K_2O	0.88
P_2O_5	0.35

7. Construct a table similar to Table 7.6 showing electronic configuration and CFSE (in terms of Δ_t) for both high-spin and low-spin states in *tetrahedral* coordination for Ti^{2+}, V^{2+}, Fe^{2+}, Co^{2+}, Ni^{2+}, and Cu^{2+}.

8. The table below gives the spectroscopically measured octahedral crystal-field splitting parameter (Δ_o) of oxides for several transition metal ions.

(**a**) For each ion below, calculate the octahedral CFSE (crystal-field stabilization energy), in joules per mole, for the high spin state. The data are given in terms of wavenumber, which is the inverse of wavelength, λ. Recall from your physics that $\lambda = c/\nu$, and that $e = h\nu$. Useful constants are: $h = 6.626 \times 10^{-34}$ joule-sec, $c = 2.998 \times 10^{10}$ cm/sec, $N_A = 6.023 \times 10^{23}$ atoms/mole.

(**b**) Assuming $\Delta_t = {}^4/_9\Delta_o$, use the table you constructed in problem 7 to calculate the tetrahedral CFSE for the high-spin state.

(**c**) Calculate the OSPE (octahedral site preference energy) for each (OSPE = Octa. CFSE − tetra. CFSE).

Ion	Δo (cm^{-1})
Ti^{2+}	16100
V^{2+}	13550
Fe^{2+}	11200
Co^{2+}	8080
Ni^{2+}	7240
Cu^{2+}	12600

9. Calculate the relative concentrations (i.e., C^l/C^o) in a partial melt at increments of F = 0.1, under the following assumptions:

(**a**) Homogenous solid phase, equilibrium (batch) melting for D = 0.01 and D = 10.
(**b**) Calculate the relative concentration in the aggregate liquid for fractional melting for D = 0.01 and D = 10.
(**c**) Plot C^l/C^o vs. F for a and b on the same graph, labeling each curve (use different colors or line types as well).

10. Calculate the enrichment of rare earth elements in an equilibrium partial melt of a mantle consisting of 10% cpx, 5% gar, 25% opx and 60% ol, assuming *modal* (phases enter the melt in the same proportion as they exist in the solid) melting for F = 0.02 and F = 0.10. Assume the concentrations in the mantle are chondritic. Use the partition coefficients given in Table 7.5. *Where data are missing in this table, interpolate the values of partition coefficients*. Use only the following eight rare earths: La, Ce, Nd, Sm, Eu, Gd, Dy, and Lu. Plot the results on a semi-log plot of chondrite-normalized abundance versus atomic number (i.e. typical REE plot). Draw a smooth curve through the REE, interpolating the other REE. (*Hint: work only with chondrite-normalized abundances, don't worry about absolute concentrations, so the* C^o *values will all be 1*.)

11. Calculate the relative enrichments of La and Sm and the La/Sm ratio in an aggregate melt produced by continuous melting. Assume bulk distribution coefficients for these two elements of 0.01 and 0.05 respectively. Do the calculation for porosities (ϕ) of 0.001 and 0.01.

(**a**) Plot your results as a function of extent of melting, F, letting F vary from 0.001 to 0.1.
(**b**) Plot your results on a process identification diagram, i.e., plot La/Sm vs. La, assuming initial La and Sm concentrations of 1.
(**c**) Do the same calculation for and batch melting. Compare the two processes, aggregate continuously and batch on a plot of plot La/Sm vs. La.

12. Calculate the change in the La/Sm ratio of a melt undergoing *in situ* crystallization assuming bulk partition coefficients for La and Sm of 0.05 and 0.2 respectively. Assume the melt initially has a La/Sm ratio of 1. Do the calculation for values of f of 0.05 and 0.25 and assume that $f_A = f$.

(**a**) Plot your results as a function of $M^l/M°$.
(**b**) Plot your results on a process identification diagram, i.e., plot La/Sm vs. La, assuming initial La and Sm concentrations of 1.

Chapter 8

Radiogenic isotope geochemistry

8.1 INTRODUCTION

Radiogenic isotope geochemistry had an enormous influence on geologic thinking in the 20th century. The story began, however, in the late 19th century. At that time Lord Kelvin (born William Thomson, and who profoundly influenced the development of physics and thermodynamics in the 19th century) estimated the age of the solar system to be about 100 million years, based on the assumption that the Sun's energy was derived from gravitational collapse. In 1897 he revised this estimate downward to the range of 20 to 40 million years. A year earlier, another Englishman, John Jolly, estimated the age of the Earth to be about 100 million years based on the assumption that salts in the ocean had built up through geologic time at a rate proportional to their delivery by rivers. Geologists were particularly skeptical of Kelvin's revised estimate, feeling the Earth must be older than this, but had no quantitative means of supporting their arguments. They did not realize it, but the key to the ultimate solution of the dilemma, radioactivity, had been discovered about the same time (1896) by Frenchman Henri Becquerel. Only 11 years elapsed before Bertram Boltwood, an American chemist, published the first "radiometric age". He determined the lead concentrations in three samples of pitchblende, a uranium ore, and concluded they ranged in age from 410 to 535 million years. In the meantime, Jolly also had been busy exploring the uses of radioactivity in geology and published what we might call the first book on isotope geochemistry in 1908. When the dust settled, the evidence favoring an older Earth was deemed conclusive.

Satisfied though they might have been with this victory, geologists remained skeptical of radiometric age determinations. One exception was Arthur Holmes, who in 1913 estimated that the oldest rocks were at least 1600 million years old (Holmes was exceptional also in his support for Alfred Wegener's hypothesis of continental drift). Many geologists were as unhappy with Holmes's age for the Earth as they had been with Kelvin's.

Until the end of World War II, the measurement of isotope ratios was the exclusive province of physicists. One name, that of Alfred Nier, stands out over this period. Nier determined the isotopic compositions of many elements and made the first measurements of geologic time based on isotope ratios rather than elemental abundances. Modern mass spectrometers, while vastly more sophisticated than those of a half century ago, have evolved from Nier's 1940 design. After World War II, mass spectrometers began to appear in geologic laboratories. Many of these laboratories were established by former students and associates of Nier or Harold Urey of the University of Chicago. As this occurred,

Geochemistry, First Edition. William M. White.
© 2013 John Wiley & Sons, Ltd. Published 2013 by John Wiley & Sons, Ltd.

isotope geochemistry expanded well beyond geochronology, ultimately to have an impact in almost every branch of earth science.

Beyond providing precise ages of geologic events, radioactive decay is important because it provides natural tracers of geologic processes and because it provides information on the rates and pathways of geologic evolution. To understand the first point, consider a biologist who wishes to know how a nutrient, phosphorus for example, is utilized by an organism, a horse for example. The biologist can feed the horse grain doped with a small amount of radioactive phosphorus. Then by taking tissue and fluid samples and determining the amount of radioactive phosphorus present, he can trace phosphorus through various metabolic pathways. Similarly, an engineer might test a new automobile design by placing a model in a wind tunnel and using smoke as a tracer to follow the path of air around it. In principle at least, we could do a similar thing with the Earth. We might add dye to downwelling ocean water to trace deep ocean currents, or add a radioactive tracer to subducting lithosphere to trace mantle convection currents. In practice, however, even the contemplation of such experiments is a bit absurd. We would need far too much dye or radioactive tracer: the scales of distance and mass are simply too large for this kind of experiment. Even if we could overcome that obstacle, we would be long dead before any useful results came from our experiment: the rates of geologic processes are simply too slow.

Nature, however, has provided natural tracers in the form of the radiogenic isotopes, which are products of natural radioactivity, and these tracers have been moving through the Earth since its beginning. For example, subducting oceanic crust has a different ratio of ^{87}Sr to ^{86}Sr than does the mantle, so we can use the $^{87}Sr/^{86}Sr$ ratio to trace the flow of subducting lithosphere through the mantle. Similarly, Atlantic water has a lower $^{143}Nd/^{144}Nd$ ratio than does Pacific water, so we can trace the flow of North Atlantic Deep Water into the Pacific using the $^{143}Nd/^{144}Nd$ ratio.

To understand the second point, consider the continental crust, which has a much higher ratio of Rb to Sr than does the mantle. Through time, this has led to a higher ratio of ^{87}Sr, the product of radioactive decay of ^{87}Rb, to ^{86}Sr in the crust than the mantle. However, the $^{87}Sr/^{86}Sr$ ratio in crustal rocks is lower than it should be had these rocks had their present Rb/Sr ratio for 4500 million years. From this observation we can conclude that the crust has not existed, or at least has not had its present composition, for the full 4500 million year history of the Earth. The situation is just the opposite for the mantle: had it had its present Rb/Sr ratio for 4500 million years it should have a lower $^{87}Sr/^{86}Sr$ than it does. Apparently, the mantle has had a higher Rb/Sr ratio in the past. From these simple observations we can draw the inference that the crust has evolved from the mantle through time. With more quantitative observations we can use isotope ratios to estimate the *rate* of crustal evolution.

Two fundamental assumptions are involved in virtually all geologic uses of radiogenic isotope ratios. The first is that the rate of radioactive decay is independent of all external influences, such as temperature and pressure. The second is that two isotopes of the same element are chemical identical and therefore that chemical processes cannot change, or fractionate, the ratio of two isotopes of the same elements. Neither of these assumptions holds in the absolute.* Nevertheless, all available evidence indicates that violations of these assumptions are entirely negligible.

8.2 PHYSICS OF THE NUCLEUS AND THE STRUCTURE OF NUCLEI

Nuclear physics is relevant to geochemistry for two reasons. First, the study of the distribution of isotopes forms an increasingly important part of geochemistry as well as

* There is a slight dependence of the rate of electron capture on pressure, and at extreme temperatures where nuclei become thermally excited there could be a dependence of decay rate on temperature (such temperatures, however, will only occur in the interiors of stars). There are subtle differences in the chemical behavior of the different isotopes of an element, which can be exploited for geologic use, as we shall see in the next chapter. For most radiogenic elements, "isotopic fractionations" are small and corrections for them are easily and routinely made.

earth science generally. Second, geochemistry concerns itself not only with the distribution of elements, but also with their origin, and the elements originated through nuclear processes, a topic we will consider in Chapter 10.

Nuclei are made up of various numbers of neutrons and protons. We'll use N to represent the number of neutrons, the *neutron number*, and Z to represent the number of protons, or *proton number*. Z is also the *atomic number* of the element, because the chemical properties of elements depend almost exclusively on the number of protons (since in the neutral atom the number of electrons equals the number of protons). The sum of Z and N is the mass number A.

8.2.1 Nuclear structure and energetics

Not all possible combinations of protons and neutrons result in stable nuclei. Typically for stable nuclei, $N \approx Z$. Thus a significant portion of the nucleus consists of protons, which tend to repel each other. From the observation that nuclei exist at all, it is apparent that another force must exist that is stronger than coulomb repulsion at short distances. It must be negligible at larger distances, otherwise all matter would collapse into a single nucleus. This force, called the nuclear force, is a manifestation of one of the fundamental forces of nature (or a manifestation of the single force in nature if you prefer unifying theories), called the *strong* force. If this force is assigned a strength of 1, then the strengths of other forces are: electromagnetic 10^{-2}; weak force 10^{-5}; gravity 10^{-39} (we will discuss the weak nuclear force shortly). Just as electromagnetic forces are mediated by a particle, the photon, the nuclear force is mediated by the pion. The photon carries one quantum of electromagnetic force field; the pion carries one quantum of nuclear force field. The strong force also binds quarks together to form hadrons, a class of particles that includes neutrons and protons. The intensity of the strong force decreases rapidly with distance, so that at distances of more than about 10^{-14} m it is weaker than the electromagnetic force.

One of the rules of thermodynamics is that the configuration with the lowest Gibbs free energy is the most stable. This is really just one example of the general physical principle that the lowest energy configuration is the most stable; this rule applies to electron orbital configurations, as we saw in crystal field theory, and to nuclei. We would thus expect that if ^{4}He is stable relative to two free neutrons and two free protons, ^{4}He must be a lower energy state compared with the free particles. If this is the case, then from Einstein's mass–energy equivalence:

$$E = mc^2 \tag{8.1}$$

we can predict that the ^{4}He nucleus will have less mass than two free neutrons and two free protons. It does in fact have less mass. From the principle that the lowest energy configurations are the most stable and the mass–energy equivalence, we should be able to predict the relative stability of various nuclei from their masses alone.

We begin by calculating the nominal weight of an atom from the sum of the mass of the constituent particles:

Proton: 1.007276 u or Da* = $1.6726218 \times 10^{-27}$ kg = 938.272 MeV/c^2
Neutron: 1.008664 u = $1.67492735 \times 10^{-27}$ kg = 939.765 MeV/c^2
Electron: 0.00054858 u = $9.1093829 \times 10^{-31}$ kg = 0.5109889 MeV/c^2

Then we define the *mass decrement* of an atom as:

$$\delta = W - M \tag{8.2}$$

* The atomic unit of mass was formerly called an *atomic mass unit* or *amu*, but it now called the unified atomic mass unit and abbreviated *u*. It is defined as a twelfth of the mass of a ^{12}C atom. 1 u = $1.6605389 \times 10^{-27}$ kg. This same unit is also sometimes called the *Dalton*, abbreviated *Da*. The international organization in charge of units and measures, the *Comité international des poids et mesures* (CIPM), has declared that *u*, not *Da*, is the official SI unit. However, use of the Dalton remains common in biochemistry. Physicists sometimes find it useful to speak of the equivalent rest energy of elementary particles, calculated from eqn. 8.1. Strictly speaking, these have units of energy divided by the speed of light, e.g., MeV/c^2. Physicists, however, often just refer to these masses as MeV.

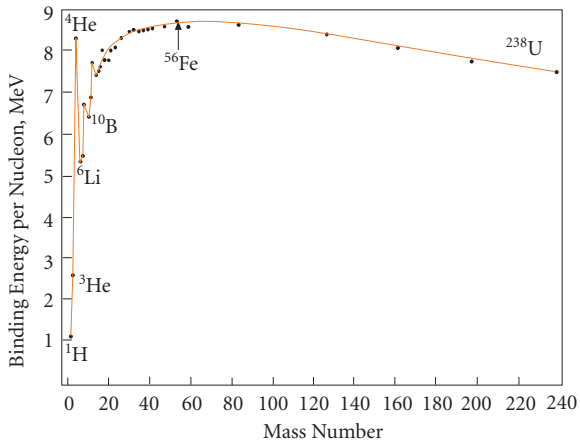

Figure 8.1 Binding energy per nucleon versus mass number.

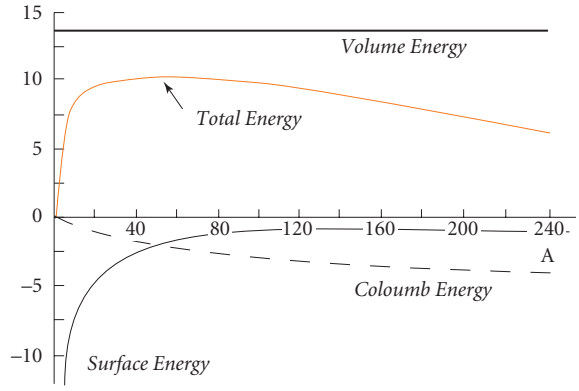

Figure 8.2 Binding energy per nucleon versus mass number as calculated using Bohr's liquid-drop experiment.

where W is the sum of the mass of the constituent particles and M is the actual mass of the atom. For example, W for ^{4}He is: $W = 2m_p + 2m_n + 2m_e = 4.03297$ u. The mass of ^{4}He is 4.002603 u, so $\delta = 0.030306$ u. Converting this to energy using eqn. 8.1 yields 28.29 MeV. This energy is known as the *binding energy*. Dividing by A, the mass number, or number of nucleons, gives the *binding energy per nucleon*, E_b:

$$E_b = \frac{W - M}{A} c^2 \qquad (8.3)$$

E_b is a measure of nuclear stability: those nuclei with the largest binding energy per nucleon are the most stable. Figure 8.1 shows E_b as a function of mass. Note that the nucleons of intermediate mass tend to be the most stable.

Some indication of the relative strength of the nuclear binding force can be obtained by comparing the mass decrement associated with it to that associated with binding an electron to a proton in a hydrogen atom. The mass decrement above is of the order of 1%, 1 part in 10^2. The mass decrement associated with binding an electron to a nucleus is of the order of 1 part in 10^8, so bonds between nucleons are about 10^6 times stronger than bonds between electrons and nuclei.

Why are some combinations of N and Z more stable than others? The answer has to do with the forces between nucleons and how nucleons are organized within the nucleus. The structure and organization of the nucleus are questions still being actively researched in physics, and full treatment is certainly beyond the scope of this book, but we can gain some valuable insight to nuclear stability by considering two of the simplest models of nuclear structure. The simplest model of the nucleus is the *liquid-drop model*, proposed by Niels Bohr in 1936. This model assumes all nucleons in a nucleus have equivalent states. As its name suggests, the model treats the binding between nucleons as similar to the binding between molecules in a liquid drop. According to the liquid-drop model, three effects influence the total binding of nucleons: a volume energy, a surface energy, and a coulomb energy. The variation of these three forces with mass number and their total effect is shown in Figure 8.2.

Looking again at Figure 8.1, we see that, except for very light nuclei, the binding energy per nucleon is roughly constant, or that total binding energy is roughly proportional to the number of nucleons. Similarly, for a drop of liquid, the energy required to evaporate it, or unbind the molecules, would be proportional to the volume of the liquid. So the volume effect contributes a constant amount of energy per nucleon.

The surface effect arises from saturation of the strong nuclear force: a nucleon in the interior of the nucleus is surrounded by other nucleons and exerts no force on more distance nucleons. But at the surface, the force is unsaturated, leading to a force similar to surface tension in liquids. This force tends to

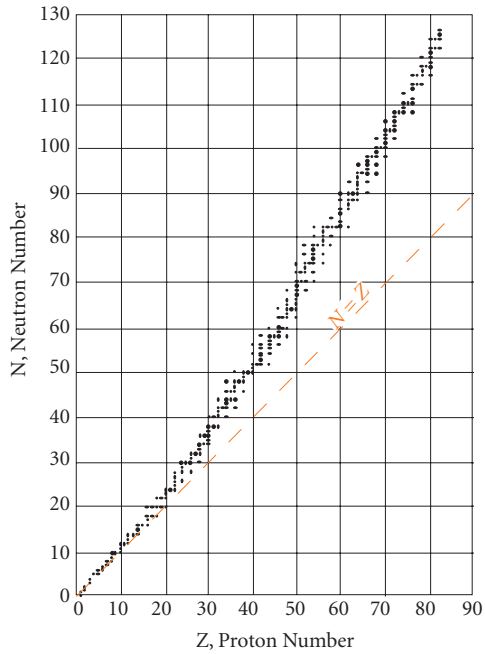

Figure 8.3 Neutron number versus proton number for stable nuclides.

minimize the surface area of the nucleus. The surface force is strongest for light nuclei and becomes rapidly less important for heavier nuclei.

The third effect on nuclear stability considered by the liquid-drop model is the repulsive force between protons. This force is a longer range one than the strong force and does not show saturation. It is proportional to the total number of proton pairs ($Z(Z-1)/2$) and inversely proportional to radius. Figure 8.3 shows the stable combinations of N and Z on a plot of N against Z. Clearly, for light isotopes, N must roughly equal Z for a nucleus to be stable. For heavier isotopes, the field of stability moves in the direction of $N > Z$. This effect may also be explained by the repulsive Coulomb force of the protons. The additional neutrons act to dilute the charge density (increase the radius) and thereby increase stability.

The liquid-drop model can account for the general pattern of binding energy in Figure 8.1 and the general distribution of stable nuclei in Figure 8.3, but not the details. The model predicts a smooth variation in binding energy with mass number, but it is apparent from Figure 8.1 that this is not the case:

Table 8.1 Numbers of stable odd and even nuclei.

Z	N	A (Z + N)	Number of stable nuclei	Number of very long-lived nuclei
Odd	Odd	Even	4	5
Odd	Even	Odd	50	3
Even	Odd	Odd	55	3
Even	Even	Even	165	11

certain maxima occur and some configurations are more stable than others. From this, we might guess that the nucleus has some internal structure.

Another interesting observation is the distribution of stable nuclei. Nuclei with even numbers of protons and neutrons are more stable than those with odd numbers of protons or neutrons. As Table 8.1 shows, stable even–even configurations are most common; stable odd–odd configurations are particularly rare. In addition, as can be seen in Figure 8.3, stable nuclei seem to be particularly common at *magic numbers*, that is, when either N or Z equals 2, 8, 20, 28, 50, 82, and 126. These observations, the even number and magic number effects, led to the *shell model of the nucleus*. It is similar to the shell model of electron structure and is based on the same physical principles, namely the Pauli exclusion principle and quantum mechanics. The Pauli exclusion principle says that no state occupied by one nucleon can be occupied by another nucleon; a nucleon added to a nucleus must occupy a new state, or niche.

These states can be described by quantum numbers. One of these quantum numbers is spin. Two protons can have the same spatial quantum numbers if their spins are antialigned (the situation is analogous to electrons sharing orbits). This is also true of neutrons. Apparently, nuclei are more stable when spins cancel (i.e., even number of protons or neutrons). The first proton and neutron shells are filled when occupied by two nucleons each. As in the atomic model, filling these shells produces a particularly stable configuration. The next shells are filled when 6 additional protons and neutrons are added for a total of 8 (each). This configuration is ^{16}O. And so on, shells being filled with 2, 8,

20, 28, 50, 82, and 126 nucleons. These numbers of nucleons, which correspond to particularly stable nuclei, were called "magic numbers" and were an important clue leading to the shell model.

Another important aspect of the shell model is its prediction of nuclear angular momentum. Even–even nuclei have no angular momentum because spins of the neutrons cancel by anti-alignment, as do the proton spins. And the angular orbital momentum is zero because the nucleons are in closed shells. In even–odd and odd–even nuclides, one odd nucleon combines its half-integral spin with the integral orbital angular momentum quantum number of the nucleus, yielding half-integral angular momentum. In odd–odd nuclei, the odd proton and odd neutron each contribute a spin of ½, yielding an integral angular momentum, which can combine with an integral orbital angular momentum quantum number to produce an integral angular momentum.

A slightly more complex model is called the *collective model*. It is intermediate between the liquid-drop and the shell models. It emphasizes the collective motion of nuclear matter, particularly the vibrations and rotations, both quantized in energy, in which large groups of nucleons can participate. Even–even nuclides with Z or N close to magic numbers are particularly stable with nearly perfect spherical symmetry. Spherical nuclides cannot rotate because of a dictum of quantum mechanics that a rotation about an axis of symmetry is undetectable, and hence cannot exist, and in a sphere every axis is a symmetry axis. The excitation of such nuclei (that is, when their energy rises to some quantum level above the ground state) may be ascribed to the vibration of the nucleus as a whole. On the other hand, even–even nuclides far from magic numbers depart substantially from spherical symmetry and the excitation energies of their excited states may be ascribed to rotation of the nucleus.

8.2.2 The decay of excited and unstable nuclei

Just as an atom can exist in any one of a number of excited states, so too can a nucleus have a set of discrete, quantized, excited nuclear states. The behavior of nuclei in transforming to more stable states is somewhat similar to atomic transformation from excited to more stable sites, but there are some important differences. First, energy level spacing is much greater; second, the time an unstable nucleus spends in an excited state can range from 10^{-14} sec to 10^{11} years, whereas atomic lifetimes are usually about 10^{-8} sec; third, excited atoms emit photons, but excited nuclei may emit other particles as well as photons. The photon emitted through the decay of unstable nuclei is called a gamma ray. Nuclear reactions must obey general physical laws, conservation of momentum, mass–energy, spin, and so on, and conservation of nuclear particles. In addition to the decay of an excited nucleus to a more stable state, it is also possible for an unstable nucleus to decay to an entirely different nucleus, through the emission or absorption of a particle of non-zero rest mass.

Nuclear decay takes place at a rate that follows the law of radioactive decay. Interestingly, the decay rate is dependent only on the nature and energy state of the nuclide. It is independent of the past history of the nucleus, and essentially independent of external influences such as temperature, pressure, and so on. Also, it is impossible to predict when a given nucleus will decay. We can, however, predict the probability of its decay in a given time interval. The probability of decay of a nucleus in some time interval, dt, is λ, where λ is called the decay constant. The probability of a decay among some number, N, of nuclides within dt is λN. Therefore, the rate of decay of N nuclides is:

$$\boxed{\frac{dN}{dt} = -\lambda N} \tag{8.4}$$

The minus sign simply indicates that N decreases with time. Equation 8.4 is a first-order rate law that we will call the *basic equation of radioactive decay*. It is very much analogous to rate equations for chemical reactions (Chapter 5), and in this sense λ is exactly analogous to k, the rate constant, for chemical reactions, except that λ is independent of all other factors.

8.2.2.1 Gamma decay

Gamma emission occurs when an excited nucleus decays to a more stable state. A

gamma ray is simply a high-energy photon (i.e., electromagnetic radiation). Its frequency, ν, is related to the energy difference by:

$$h\nu = E_u - E_l \qquad (8.5)$$

where E_u and E_l are the energies of the upper (excited) and lower (ground) states and h is Planck's constant. The nuclear reaction is written as:

$$^{N}Z^{*} \rightarrow {}^{N}Z + \gamma \qquad (8.6)$$

where Z is the element symbol, N is the mass number, and γ denotes the gamma ray.

8.2.2.2 *Alpha decay*

An α-particle is simply a helium nucleus. Since the helium nucleus is particularly stable, it is not surprising that such a group of particles might exist within the parent nucleus before α-decay. Emission of an alpha particle decreases the mass of the nucleus by the mass of the alpha particle plus a mass equivalent to the energy lost during the decay, which includes the kinetic energy of the alpha particle (constant for any given decay) and the remaining nucleus (because of the conservation of momentum, the remaining nucleus recoils from the decay reaction), and any gamma ray emitted.

The escape of the α particle is a bit of a problem, because it must overcome a very substantial energy barrier, a combination of the strong force and the coulomb repulsion, to get out. For example, α particles with energies below 8 MeV are scattered from the ^{238}U nucleus. However, the α particle emerges from the decaying ^{238}U with an energy of only about 4 MeV. This is an example of a quantum mechanical effect called *tunneling* and can be understood as follows. Quantum mechanics holds that we can never know exactly where the α particle is (or any other particle, or you or I for that matter), we only the know the probability of its being in a particular place. This probability is determined by the square of the particle's wave function, ψ. Although the wave is strongly attenuated through the potential energy barrier, it nevertheless has a small but finite amplitude outside the nucleus, and hence there is a small but finite probability of the α particle being located outside the nucleus. Anything that can occur ultimately will, so sooner or later the alpha particle escapes the nucleus.

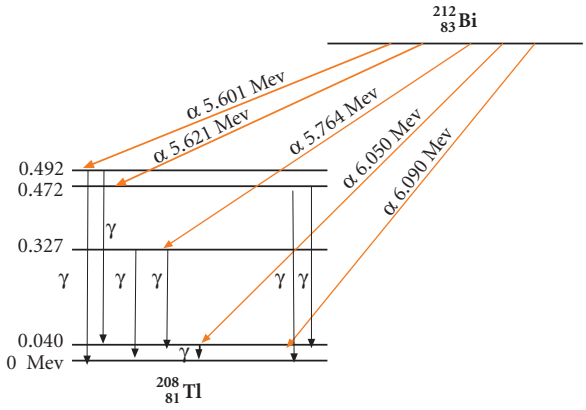

Figure 8.4 Nuclear energy-level diagram showing decay of bismuth-212 by alpha emission to the ground and excited states of thallium-208.

The daughter may originally be in an excited state, from which it decays by γ decay. Figure 8.4 shows an energy-level diagram for such a decay.

Alpha-decay occurs in nuclei with masses above the maximum in the binding energy curve of Figure 8.1, located at ^{56}Fe. Quite possibly, all such nuclei are unstable relative to alpha-decay, but the half-lives of most of them are immeasurably long.

8.2.2.3 *Beta decay*

Beta decay is a process in which the charge of a nucleus changes, but not the number of nucleons. If we plotted Figure 8.3 with a third dimension, namely energy of the nucleus, we would see that stable nuclei are located in an energy valley. Alpha-decay moves a nucleus down the valley axis; beta decay moves a nucleus down the walls toward the valley axis. Beta-decay results in the emission of an electron or positron (a positively charged electron), depending on which side of the valley the parent lies. Consider the three nuclei in Figure 8.5. These are known as *isobars*, since they have the same number of nucleons (12; *isotopes* have the same number of protons, *isotones* have the same number of neutrons). From what we know of nuclear structure, we can predict that the ^{12}C nucleus is the most

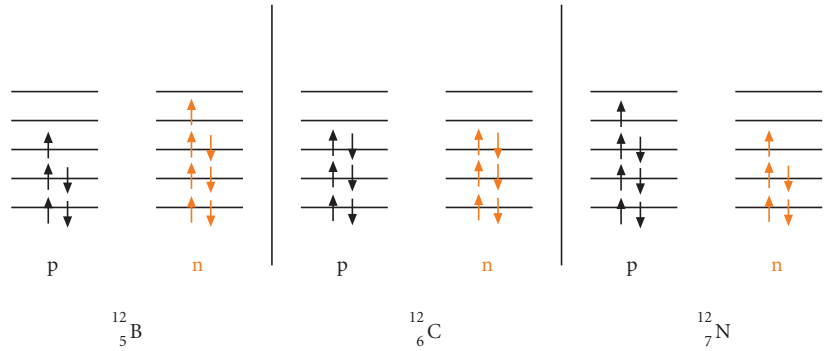

Figure 8.5 Proton and neutron occupation levels of boron-12, carbon-12 and nitrogen-12.

stable of these three, because the spins of the neutrons and protons cancel each other. This is the case: ^{12}B decays to ^{12}C by the creation and emission of a β^- particle and the conversion of a neutron to a proton. ^{12}N decays by emission of a β^+ and conversion of a proton to a neutron.

The discovery of beta decay presented physicists with a problem. Angular momentum must be conserved in the decay of nuclei. The ^{12}C nucleus has integral spin, as do ^{12}B and ^{12}N. But the beta particle (an electron or positron) has ½ quantum spin units, hence β decay apparently resulted in the loss of ½ spin units. The solution, proposed by Enrico Fermi,* was another, essentially massless particle called the *neutrino*, with ½ spin to conserve angular momentum. (It is now known that neutrinos do have mass, albeit a very small one that has not yet been directly measured. Other theoretical constraints require the neutrino mass to be somewhere between 0.5 eV and 0.05 eV; comparing this with the electron mass of about 0.5 MeV, we see it is roughly 10^{-6} to 10^{-7} smaller.) It is also needed to balance energy. The kinetic energies of alpha particles are discrete. Not so for betas: they show a spectrum with a characteristic maximum energy for a given decay. Since energy must be conserved, and the total energy given off in any decay must be the same, it is apparent that the neutrino must also carry away part of the energy. The exact distribution of energy between the beta and the neutrino is random: it cannot be predicted in an isolated case, though there tends to be a fixed statistical distribution of energies, with the average observed beta energies being about a third the maximum value (the maximum value is the case where the beta carries all the energy).

Beta decay involves the weak nuclear force. The weak force transforms a neutral particle into a charged one and visa versa. Both the weak and the electromagnetic force are now thought to be simply a manifestation of one force that accounts for all interactions involving charge (in the same sense that electrical and magnetic forces are manifestations of electromagnetism). This force is called electroweak. In β^+ decay, for example, a proton is converted to a neutron, giving up its +1 charge to a neutrino, which is converted to a positron. This process occurs through the intermediacy of the W+ particle in the same way that electromagnetic processes are mediated by photons. The photon and W particles are members of a class of particles called *bosons* that mediate forces between the basic constituents of matter. However, W particles differ from photons in having a substantial mass.

8.2.2.4 Electron capture

Another type of reaction is electron capture. This is sort of the reverse of beta decay and has the same effect, more or less, as β^+ decay. Interestingly, this is a process in which an

* Enrico Fermi (1901–1954) had the unusual distinction of being both an outstanding theorist and an outstanding experimentalist. He made many contributions to quantum and nuclear physics and won the Nobel Prize in 1938. Interestingly, the journal *Nature* rejected the paper in which Fermi made this proposal!

Example 8.1 Calculating binding energies

Calculate the binding energies of ^{50}V, ^{50}Cr, and ^{50}Ti. Which of these three nuclei is the least stable? Which is the most stable?

Answer: the nucleus of ^{50}V consists of 23 protons and 27 neutrons, that of ^{50}Cr consists of 24 protons and 26 neutrons, that of ^{50}Ti consists of 22 protons and 28 neutrons. Atoms of these elements also have, respectively, 23, 24, and 22 electrons. First we calculate W for each:

$$W(^{50}V) = 23\times1.007276 + 27\times1.008665 + 23\times0.0005458 = 50.413856\ u$$

$$W(^{50}Cr) = 24\times1.007276 + 26\times1.008665 + 24\times0.0005458 = 50.413013\ u$$

$$W(^{50}Ti) = 22\times1.007276 + 28\times1.008665 + 22\times0.0005458 = 50.41470\ u$$

The actual masses (M) of these nuclides are: ^{50}V, 49.947163 u; ^{50}Cr, 49.94805 u; ^{50}Ti, 49.944792 u. Using eqn. 8.2 we calculate the mass decrement, and then divide by 50 to calculate the mass decrement per nucleon. We convert the result to kg using the conversion factor $1\ u = 1.6605 \times 10^{-27}$ kg. We then multiply by the square of the speed of light (2.99792×10^{8} m/sec) to obtain the binding energy in kg-m/sec or joules. We use $1\ J = 6.2415 \times 10^{12}$ MeV to convert our answer to MeV. The results are shown in the table below.

Nuclide	δ u	δ kg	δ/A kg/nucleon	E_b J/nucleon	E_b MeV
^{50}V	0.46669	7.7496×10^{-28}	1.5499×10^{-29}	1.3878×10^{-12}	8.6944
^{50}Cr	0.46493	7.7209×10^{-28}	1.5442×10^{-29}	1.3878×10^{-12}	8.6622
^{50}Ti	0.43991	7.8030×10^{-28}	1.5606×10^{-29}	1.4023×10^{-12}	8.7543

Our results indicate that of the three, ^{50}V is the least stable and ^{50}Ti the most stable, though the difference is not that great. ^{50}V is an example of a branched decay: it can decay by β^- to ^{50}Cr or ^{50}Ti by electron capture.

electron is added to a nucleus to produce a nucleus with less mass than the parent! The missing mass is carried off as energy by an escaping neutrino, and in some cases by a γ. In some cases, a nucleus can decay by either electron capture, β^-, or β^+ emission. An example is the decay of ^{40}K, which decays to ^{40}Ar by β^+ or electron capture and to ^{40}Ca by β^-. In Example 8.1, we found that ^{50}V was less stable than its two isobars: ^{50}Cr and ^{50}Ti. In fact, a ^{50}V atom will eventually decay to either a ^{50}Cr atom by β^- decay or to ^{50}Ti by electron capture. The half-life for this decay is 1.4×10^{17} years, so that the decay of any single atom of ^{50}V is extremely improbable.

β decay and electron capture often leave the daughter nucleus in an excited state. In this case, it will decay to its ground state (usually very quickly) by the emission of a γ-ray. Thus γ rays often accompany β decay. A change in charge of the nucleus necessitates a rearrangement of the electrons in their orbits. This rearrangement results in X-rays being emitted from electrons in the inner orbits.

8.2.2.5 *Spontaneous fission*

Fission is a process by which a nucleus splits into two or more fairly heavy daughter nuclei. In nature, this is a very rare process, occurring only in the heaviest nuclei, ^{238}U, ^{235}U, and ^{232}Th (it is most likely in ^{238}U). This particular phenomenon is perhaps better explained by the liquid-drop model than the shell model. In the liquid-drop model, the surface tension tends to minimize the surface area while the repulsive coulomb energy tends to increase it.

We can visualize these heavy nuclei as oscillating between various shapes. The nucleus may very rarely become so distorted by the repulsive force of 90 or so protons that the surface tension cannot restore the shape. Surface tension is instead minimized by splitting the nucleus entirely. Since there is a tendency for the N/Z ratio to increase with A for stable nuclei, the parent is neutron-rich. When fission occurs, some free neutrons are produced and nuclear fragments (the daughters, which may range from A = 30, zinc, to A = 64, terbium) are too rich in neutrons to be stable. The immediate daughters will decay by β^- decay until enough neutrons have been converted to protons that it has reached the valley of energy stability. It is this tendency to produce unstable nuclear byproducts, rather than fission itself, which makes fission in bombs and nuclear reactors such radiation hazards.

Some unstable heavy nuclei and excited heavy nuclei are particularly subject to fission. An important example is ^{236}U. Imagine a material rich in U. When one ^{238}U undergoes fission, some of the released neutrons are captured by ^{235}U nuclei, producing ^{236}U in an excited state. This ^{236}U then fissions producing more neutrons, and so on – a sustained chain reaction. This is the basis of nuclear reactors and bombs (actually, the latter more often use some other nuclei, like Pu). The concentration of U, and ^{235}U in particular, is not high enough for this sort of thing to happen naturally – fission chain reactions require U enriched in ^{235}U. However, the concentration of ^{235}U was higher in the ancient Earth and at least one sustained natural chain reaction is known to have occurred about 2 billion years ago in the Oklo uranium deposit in Gabon, Africa. This deposit was found to have an anomalously low ^{235}U/^{238}U ratio, indicating some of the ^{235}U had been "burned" in a nuclear chain reaction. Anomalously high concentrations of fission-produced nuclides confirmed that this had indeed occurred.

Individual fission reactions are less rare. When fission occurs, there is a fair amount of kinetic energy produced, the fragments literally flying apart. These fragments damage the crystal structure through which they pass, producing "tracks" whose visibility can be enhanced by etching. This is the basis of *fission track dating*.

Natural fission also can produce variations in the isotopic abundance of the daughter elements. In general, however, the amount of the daughter produced is so small relative to that already present in the Earth that these isotopic variations are immeasurably small. An important exception is xenon, whose isotopic composition can vary slightly due to contributions from fission of U and the extinct radionuclide ^{244}Pu.

8.3 BASICS OF RADIOGENIC ISOTOPE GEOCHEMISTRY

The basic equation of radioactive decay is:

$$\frac{dN}{dt} = -\lambda N \tag{8.4}$$

λ is the decay constant, which we defined as the probability that a given atom would decay in some time dt. It has units of time^{-1}. Let's rearrange eqn. 8.4 and integrate:

$$\int_{N_0}^{N} \frac{dN}{N} = \int_0^t -\lambda dt \tag{8.7}$$

where N_0 is the number of atoms of the radioactive, or parent, isotope present at time $t = 0$. Integrating, we obtain:

$$\ln \frac{N}{N_0} = -\lambda t \tag{8.8}$$

This can be expressed as:

$$\frac{N}{N_0} = e^{-\lambda t} \quad \text{or} \quad N = N_0 e^{-\lambda t} \tag{8.9}$$

Suppose we want to know the amount of time for the number of parent atoms to decrease to half the original number, that is, t when $N/N_0 = ½$. Setting N/N_0 to ½, we can rearrange eqn. (8.8) to get:

$$\ln \frac{1}{2} = -\lambda t_{1/2} \quad \text{or} \quad \ln 2 = \lambda t_{1/2}$$

and finally:

$$t_{1/2} = \frac{\ln 2}{\lambda} \tag{8.10}$$

This is the definition of the *half-life*, $t½$.

Now the decay of the parent produces some daughter, or *radiogenic*, nuclides. The